Coarsening of facetted two-dimensional islands by dynamic coalescence

V. M. Kaganer and K. H. Ploog

Paul-Drude-Institut für Festkörperelektronik, Hausvogteiplatz 5-7, D-10117 Berlin, Germany

K. K. Sabelfeld

Weierstraß-Institut für Angewandte Analysis und Stochastik, Mohrenstrasse 39, 10117 Berlin, Germany
and Institute of Computational Mathematics and Mathematical Geophysics, Russian Academy of Sciences, Lavrentiev Prospekt 6,
630090 Novosibirsk, Russia

We study the coarsening of two-dimensional (2D) vacancy islands on a crystal surface by atomic-scale kinetic Monte Carlo simulations on an ensemble of meandering islands. The Brownian motion of islands is due to the motion of atoms within the islands, with the escape of atoms from islands prohibited by the presence of a step edge barrier. We find that the diffusion of individual islands and their size distribution qualitatively change for large bond energies or low temperatures, when the islands develop straight edges (facets). The island diffusion coefficient becomes size independent and the size distribution becomes monotonously decreasing. The results of the kinetic Monte Carlo simulations are supported by numerical solutions of the Smoluchowski equations. We derive the kernel of the Smoluchowski equations for the 2D case taking into account the screening effects and find that the screening essentially alters the island size distribution.

I. INTRODUCTION

Two-dimensional (2D) islands that form on a crystal surface during epitaxial growth bring the crystal in a nonequilibrium state. When the mean island size increases (keeping the total number of atoms in all islands conserved), the density of surface steps decreases and hence the energy of the crystal is reduced. The controlled use of surface coarsening kinetics may provide a way for the fabrication of certain desired nanostructures. The coarsening process known for more than a century is Ostwald ripening.[1–3] In this process, larger islands grow at the expense of smaller ones, which shrink by emitting atoms. Relatively recently, scanning tunneling microscopy (STM) studies of metal surfaces[4–15] have revealed another coarsening process. The 2D islands perform a Brownian motion on the surface and merge when they touch one another. This process is called dynamic coalescence, to distinguish it from static coalescence that takes place during deposition, when all islands grow simultaneously and merge when they touch due to their size increase. The diffusion of islands is due to the motion of atoms inside them or along their periphery. Even islands consisting of hundreds or thousands of atoms possess notably large diffusion coefficients.

Dynamic coalescence becomes the dominant coarsening process when the detachment of atoms from the islands is prohibited. Otherwise, Ostwald ripening is a more effective coarsening mechanism. For adatom islands, the 2D island diffusion and shape equilibration during a merger proceeds by to atom diffusion along the island perimeter. Theoretical analysis[16–18] predicts a power law dependence of the island diffusion coefficient on its size

$$D_k \propto l_k^{-\alpha}. \tag{1}$$

Here, k is the number of atoms in the island, and l_k is its linear size, $l_k = \sqrt{k}$. The periphery diffusion is characterized by the exponent $\alpha = 3$. The power law (1) was confirmed in many kinetic Monte Carlo (kMC) simulations.[19–27] However, the exponent α was found to depend on temperature. Further kMC simulations[28,29] show that the facetting of the islands at low temperatures or large bond energies qualitatively alters the island shape equilibration kinetics.

For advacancy islands, the detachment of atoms is prevented by a step edge barrier that does not allow the atoms to escape onto a higher terrace. Besides atom diffusion along the island periphery, the island diffusion can be driven by detachment of atoms from the island edge with subsequent correlated or uncorrelated reattachment. These latter processes are governed by the Gibbs-Thomson relation for the equilibrium atom density at the curved step edges bounding the islands. Detachment of atoms from the island edge with subsequent correlated reattachment results in an exponent $\alpha = 2$ in Eq. (1), while uncorrelated detachment and attachment leads to $\alpha = 1$.[16–18] Thus, these exponents, just as the exponents characteristic to the Ostwald ripening process,[2,3] rely on the Gibbs-Thomson formula and, in this sense, do not distinguish between liquid and crystalline islands. The exponent α is believed to be a temperature independent quantity characteristic for each diffusion mechanism. On the other hand, the facetting of the islands at low temperatures or large bond energies influence the kinetics of adatom islands.[28,29] Concerning advacancy islands, Van Siclen noted[16] that the diffusion coefficient of facetted vacancy islands should not depend on the island size. Our aim in the present paper is to study the diffusion of facetted vacancy islands and the coarsening kinetics driven by their dynamic coalescence.

During coarsening, the average island size $L(t) = \langle l_k \rangle$ increases in time and the island size distribution shifts to larger sizes. If the diffusion coefficient D_k follows the power dependence (1) on the size, the kinetics of the island size distribution obeys kinetic scaling: the distribution does not

change if the size scales by $L(t)$, i.e., the size distribution is described by a time-independent function $F(l_k/L)$. Moreover, one can show[21,30] that the time dependence of the mean island size follows a power law, $L \propto t^\beta$, with the exponent

$$\beta = 1/(2 + \alpha) \qquad (2)$$

related to the exponent α of the diffusion coefficient.

Once the island size dependence of the diffusion coefficient is established, the coarsening kinetics can be studied with another kind of kMC simulations, with whole islands (rather than atoms) taken as unit objects.[30–32] The time scale of the coarsening process studied in this way is much larger than the characteristic time of the individual coalescence and reshaping events, so that the latter events are treated as instantaneous.

The time evolution of the island size distribution can also be described by the Smoluchowski equations. In these equations, a merger of two islands containing i and j atoms proceeds with a rate K_{ij} that can be established for various types of island motion. Knowing the size dependence of the collision rate, one can obtain the time evolution of the island size distribution.

The aim of the present work is to study the coalescence of facetted 2D islands. We perform kMC simulations on an ensemble of islands and obtain the time evolution of their mean size and distribution directly in the atomic-scale model. In contrast to previous simulations, we consider larger bond energies, so that the islands develop facets joined by rounded corners. As a reference, we also perform simulations for smaller bond energies. In that case, the islands are rounded and the kinetics are in qualitative agreement with the previous studies, with some notable differences that we discuss.

The simulations allow us to obtain size dependencies of the island diffusion coefficient within the same kMC model. We find that the diffusion coefficient of the facetted island does not depend on its size. The island size distribution is found to be substantially different from the case of rounded islands.

We numerically solve the Smoluchowski equations to obtain the island size distributions, using the island diffusion coefficients that we find in the atomistic kMC simulations. We derive the kernel of the Smoluchowski equations that takes into account the screening effects. We find that the screening is especially important in the 2D case and qualitatively changes the island size distribution.

II. KINETIC MONTE CARLO SIMULATIONS

A. Coalescence of islands

Out of the two competing coarsening mechanisms, Ostwald ripening and dynamic coalescence, Ostwald ripening is more effective if the exchange of atoms between islands is not prohibited. In the case when the loss of atoms by the island is restricted, the motion of atoms within the island or along its periphery causes Brownian motion of the island. The coarsening proceeds due to the dynamic coalescence of the islands. The conditions for dynamic coalescence are naturally met for vacancy islands in the presence of a step

edge barrier. The adatoms move within the pit but cannot escape it to the higher terrace. We perform kMC simulations starting with a coverage of 0.9 monolayer (ML) of randomly deposited atoms. They nucleate vacancy islands of 0.1 ML coverage, and we follow their kinetics.

We use the common bond-counting ansatz[33,34] for the rates of different atomic motions. The system is described by a single bond energy E_b, so that the rate of an elementary atom jumps from the initial state with n neighbors to a final state is equal to $\nu \exp(-nE_b/k_BT)$, where T is temperature and k_B is the Boltzmann constant. In our simulations, the final state is any unoccupied neighboring site on the same level. Jumps to a higher level are prohibited by imposing an infinite step edge barrier. The prefactor ν is $\nu = \nu_0 \exp(-E_D/k_BT)$, where E_D is the surface diffusion energy and $\nu_0 = 10^{13}$ s^{-1} is the frequency of atomic vibrations. The frequency ν establishes the time scale of the problem and does not influence the results in any other respect. Thus, the kinetics of the system depend on only one parameter, the ratio E_b/k_BT. We set $T=400$ K and perform kMC simulations with two bond energies $E_b=0.2$ and 0.4 eV, so that the ratio $E_b/k_BT=5.8$ and 11.6. We take the surface diffusion energy $E_D=0.2$ eV in the case $E_b=0.2$ eV and $E_D=0$ in the case $E_b=0.4$ eV, just with the aim to bring both simulations to comparable time scales. This choice does not influence results in any other respect. We use the common variable-time algorithm[35,36] of kMC simulations, which is especially effective at large bond energies. The numbers of vacancies in the islands are calculated using the algorithm of Ref. 37. We have used a 500×500 square mesh with periodic boundary conditions for simulations with the bond energy 0.2 eV, and a 300×300 mesh for simulations with the bond energy 0.4 eV. The simulation runs were repeated 30 times to obtain sufficient statistics of the island size distribution.

Figures 1(a) and 1(b) present typical intermediate states in the time evolution of the system for bond energies of 0.2 eV and 0.4 eV. One can see a qualitative difference in the shapes of the individual vacancy islands in these two images. In the case of the larger bond energy, the islands reveal facets rounded at the corners, corresponding to the equilibrium shape of 2D crystals at a given temperature.[38] In contrast, in the case of the smaller bond energy the islands are rounded. Following the time sequence of the images, we find that the islands randomly move on the surface and merge if they touch each other. Figures 1(c) and 1(d) show a sequence of snapshots in a fixed window cut out of the simulated mesh. The behavior of the islands is similar to what is observed in the STM experiments. In the case of smaller bond energy, some density of individual vacancies is present in addition to the vacancy islands. Emission of a vacancy is a possible, albeit rare, event in our model. It is possible in the presence of the infinite step edge barrier since it involves the motion of atoms within the layer. When calculating the island size distributions and the mean island sizes, these single vacancies are excluded.

Figures 2(a) and 2(b) present the time evolution of the mean linear size of the islands $L(t)$. The kMC results are shown by circles, while the continuous lines are solutions of the Smoluchowski equations, described in the following section. We define the linear size of an island as the square root
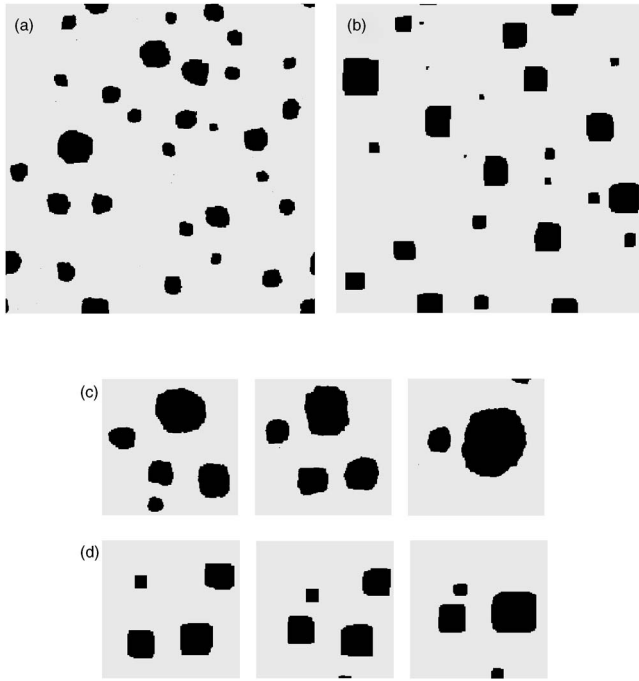
FIG. 1. Snapshots of the simulated cells for bond energies E_b =0.2 eV (a) and 0.4 eV (b), at temperature T=400 K. Vacancy islands at coverage 0.1 are simulated on a 500×500 grid in (a) and 300×300 grid in (b). The islands are rounded in (a) and facetted in (b). Brownian motion and collisions of islands are shown in (c,d).

FIG. 3. Trajectories of the mass centers of islands of linear size l=30 for bond energies E_b=0.2 eV (a) and 0.4 eV (b). The length of the scale mark is equal to the mesh period of the simulation lattice.

of the number k of vacancies in it, $l_k = \sqrt{k}$, and find the mean size $L = \langle l_k \rangle$ by averaging over the island size distribution. In the case of facetted islands, E_b=0.4 eV, the mean island size follows a power law, $L(t) \propto t^{\beta}$ with the exponent β=0.47. The behavior in the case of rounded islands, E_b=0.2 eV, is more complicated. An apparent time exponent β is size dependent: it decreases from about 0.36 for a mean island size of 10 to
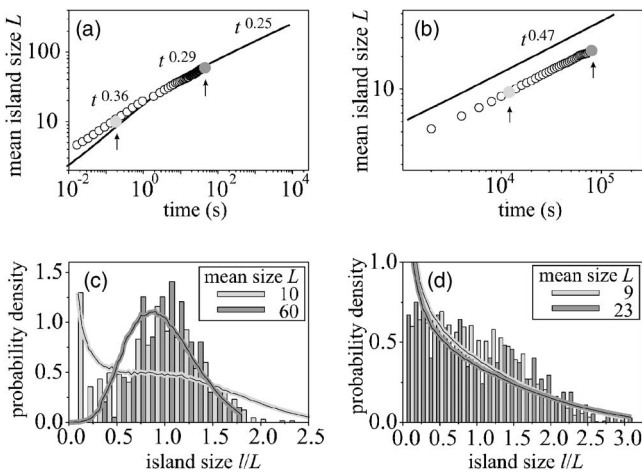

FIG. 2. Time evolution of the mean size of vacancy islands for bond energies E_b=0.2 eV (a) and 0.4 eV (b), and the respective island size distributions (c,d). Circles in (a,b) and bars in (c,d) represent the results of kinetic Monte Carlo simulations. Full lines are the solutions of the Smoluchowski equations. The size distributions in (c,d) are taken at the time moments marked in (a,b).
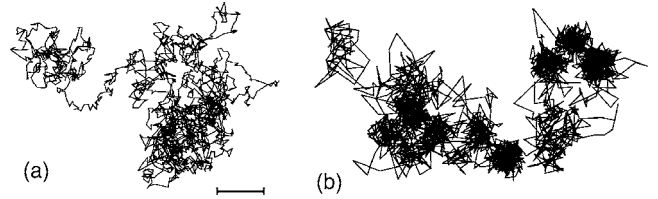
approximately 0.29 for an island size of 50. We postpone further analysis and the comparison with the numerical solution of the Smoluchowski equations [shown by lines in Figs. 2(a) and 2(b)] to Sec. IV.

The island size distributions are substantially different for the two bond energies under investigation, see Figs. 2(c) and 2(d). The distribution of rounded islands at E_b=0.2 eV is peaked at the mean island size. The contribution of individual vacancies is not shown, since the vacancies are excluded when calculating the mean size, as discussed above. For facetted islands, the kMC calculations give a broad monotonously decreasing distribution, Fig. 2(d), in contrast to the peaked distribution for rounded islands in Fig. 2(c). Further analysis of the kMC simulations is given in Sec. IV, using the simulations of individual island diffusion presented below.

B. Brownian motion of individual islands

With the aim to understand the behavior of the ensemble of islands, we perform kMC simulations of the Brownian motion of individual islands in the framework of the same model. We put a single island consisting of a given number of vacancies k and record the position of its center of mass $\mathbf{r}_k(t)$. The initial shape of the island does not play a role, since the shape equilibration proceeds much faster than the island motion. The vacancy islands move due to the motion of atoms inside them, in particular, by detachment of an atom from the island perimeter, its diffusion in the island, and subsequent reattachment at another place. Figure 3 shows typical trajectories of the centers of mass of islands of the same size, l=30, for the two energies under consideration. The trajectory for the smaller bond energy E_b=0.2 eV, Fig. 3(a), is common for Brownian motion. In the case of a larger bond energy E_b=0.4 eV, Fig. 3(b), the trajectory consists of discrete jumps with extended fluctuations of the mass center position after each jump. The jumps are rare events. They occur when an atomic row at a facet erodes by emitting atoms that build an atomic row at another facet and advance the island. The fluctuations are due to detachments of atoms from rounded corners with subsequent attachments to other corners, without moving the facets.

The mean-square displacements of the center of mass, averaged over time intervals much larger than the jumps in Fig. 3(b), depend linearly on time, indicating the Brownian character of the motion. We obtain the diffusion coefficients D_k from the averages $\langle [\mathbf{r}_k(t+\Delta t) - \mathbf{r}_k(t)]^2 \rangle = 4 D_k \Delta t$. In the
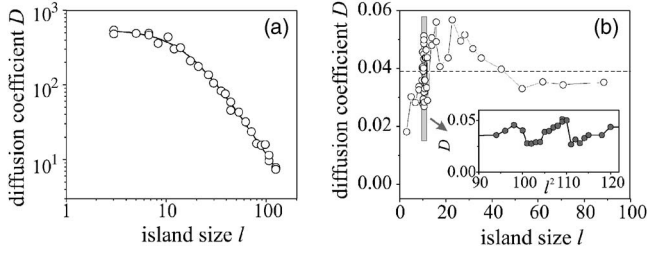
FIG. 4. Island size dependence of the diffusion coefficient for bond energies $E_b=0.2$ eV (a) and 0.4 eV (b). The insert in (b) magnifies a small size interval. Note that the insert shows the diffusion coefficient versus the number of atoms in an island, while in the other plots the linear island size is used.

case of the bond energy $E_b=0.2$ eV, we take care of the detachment of vacancies from the island. The simulation run is interrupted if detachment take place, and a new run is started. In the case of the bond energy $E_b=0.4$ eV, the detachment is negligible. An average over 50 runs is taken to have a good accuracy in the determination of D_k.

Figures 4(a) and 4(b) present the size dependence of the diffusion coefficient for the two bond energies under consideration. As above, we use the case of rounded islands at $E_b=0.2$ eV as a reference. The diffusion coefficient of large rounded islands, Fig. 4(a), exhibits the $D_k \propto l_k^{-2}$ dependence characteristic for correlated detachment and reattachment of atoms. This is the dependence described theoretically[16–18] and observed in kMC simulations[21,23–25,39] and STM experiments.[6,9,11,13,15]

The diffusion coefficient deviates from the power law for small islands. Such a deviation, to smaller values for vacancy islands[23,39] and to larger values for adatom islands,[22,24] has also been observed in the previous kMC simulations. The deviation can be explained[40] by recalling that the power law dependence (1) is obtained by taking the Gibbs-Thomson chemical potential proportional to the curvature of the island perimeter, $\mu_k=2a^2\gamma/k_BTl_k$. Here $l_k/2$ is the island radius, a^2 is the area per atom, and γ is the line tension, in our model $\gamma=E_b/a$. This expression for the chemical potential is the first term in the expansion of the Gibbs-Thomson potential $\mu_k=\exp(\mp 2a^2\gamma/k_BTl_k)$ applicable when the curvature is small enough. The two signs correspond to adatom and vacancy islands, respectively. If this condition is not fulfilled, one can consider an effective size-dependent exponent[40] $\alpha=\alpha_0 \pm 2a^2\gamma/k_BTl_k$, where α_0 is the limiting value for large islands, that depends on the diffusion mechanism. A characteristic length obtained by requiring that the argument of the exponential function is equal to 1 is, for the conditions of Fig. 4(a), $l_k/a=2E_b/k_BT=11.6$. It agrees well with the kMC results in Fig. 4(a). We find that the size dependence of the diffusion coefficient is well interpolated by the formula $D_k=D_0/[1+(l_k/l_0)^2]$, or equivalently

$$D_k = D_0/(1 + k/k_0). \tag{3}$$

The corresponding curve calculated with the value $k_0=234$ obtained by a fit is shown in Fig. 4(a) together with the kMC results.

The size dependence of the island diffusion coefficient in the case of facetted islands is completely different, see Fig. 4(b). The diffusion coefficient D_k does not decrease with increasing island size. Rather, it tends to a constant. For smaller islands, we find notable variations of D_k. These variations are not random and are much larger than a statistical error in determination of D_k for a given island size. The insert in Fig. 4(b) magnifies a small size range that we explored in detail. The diffusion coefficient systematically increases and decreases, depending on the exact number of vacancies in a cluster. In this insert, the diffusion coefficient is plotted as a function of the number of vacancies in the cluster, $k=l^2$. The variation of D_k is obviously correlated with the possibility to form a rectangular island with the sizes of integer length (10×10, 10×11, etc.). These variations are not relevant for our study of the kinetics of an ensemble of islands of different sizes and we take D_k as constant in further analysis. Thus, the facet erosion starts at a corner and its probability does not depend on the island size, which leads to a size-independent diffusion coefficient.[16] The case of a constant diffusion coefficient is described by Eq. (1) with $\alpha=0$, and hence Eq. (2) gives the time exponent of the mean island size $\beta=1/2$. This is in agreement with the kMC results, Fig. 2(b), which give $\beta=0.47$.

III. SOLUTION OF THE SMOLUCHOWSKI EQUATIONS

A. Numerical solution method

The kinetics of an ensemble of islands that diffuse on the surface and irreversibly merge as they touch each other can be described by the set of Smoluchowski equations[30–32,41]

$$dn_k/dt = \frac{1}{2}\sum_{i+j=k} K_{ij}n_i n_j - n_k\sum_{j=1}^{\infty} K_{jk}n_j. \tag{4}$$

Here n_j is the number of islands containing j units (vacancies in our case) per unit area. The first term on the right-hand side describes the formation of islands of size k by the coalescence of pairs of smaller islands and the second term represents the removal of islands of size k by coalescence with islands of all other sizes.

In the case of a general kernel K_{ij}, the Smoluchowski equations (4) have to be solved numerically. This is not trivial, since one has to solve a system of tens of thousands of coupled nonlinear ordinary differential equations. Conventional finite difference and finite element methods can be used,[42,43] however they often face the dimension problem, and hence have to introduce additional *a priori* assumptions about the tail of the size distribution for large clusters and the structure of the coagulation coefficients.

The Monte Carlo methods developed for solving the Smoluchowski equations are free of such assumptions.[44,45] Moreover, these methods adopt well to complicated kernels and inhomogeneous problems (i.e., when the kernel depends on time or spatial variables).[45,46] In this stochastic simulation approach, the system of particles is considered as a jump Markov process, which starts from the initial size distribution $n_k(0)$ and changes its state at random times, when collisions of any two particles happen. The random time has an

exponential distribution with a parameter depending on the current state of the Markov chain. The collision between two clusters of size i and size j is simulated as a random event, according to a probability distribution which is proportional to the coagulation kernel K_{ij}.

Here we formulate the simplest version of the stochastic algorithm for solving the Smoluchowski equations.[44,45] To obtain probabilities, we define a constant K_{max} that is larger than $\max\{K_{ij}\}$ over the current size distribution. Then, given the state of the system at time t_k, its state at time t_{k+1} is evaluated as follows.

(1) Simulate a random time interval Δt according to the exponential distribution $p(\tau) = \lambda \exp(-\lambda\tau)$, and calculate $t_{k+1} = t_k + \Delta t$. Here

$$\lambda = \frac{N(N-1)}{2N_0} K_{max},\qquad(5)$$

N_0 is the initial number of particles, $N(t)$ is the current number of particles, and $N(N-1)/2$ is the number of pairs of particles. Hence, Δt is given by $\Delta t = -(1/\lambda)\ln r$, where r is a random number uniformly distributed on $(0,1)$. In practice, when the value of N is large, the parameter λ is also large, the time step is quite small, and it is reasonable to take simply $\Delta t = 1/\lambda$.

(2) Take a pair of particles on random, and let i and j be the numbers of atoms in them.

(3) With the probability $p_{ij} = K_{ij}/K_{max}$ the particles i and j coagulate, i.e., the numbers n_i and n_j are decreased by one, the number n_{i+j} is increased by one, and the total number of particles N is decreased by one. Otherwise (i.e., with the probability $1 - p_{ij}$) the state of the system is not changed. Then, go to the next time step of the system evaluation.

When the number of clusters N decreases to say 50% of the initial number of simulated clusters, we enrich the statistics by doubling the system. It means that a copy of the current system is added to the particle system. Accordingly, N_0 and N are increased by a factor of 2. After this point, the system evolves further as described above. We start the simulations by taking all particles as monomers. Hence, the initial concentration in the Smoluchowski equations is increased by a factor θ^{-1} with respect to the physical parameter. Here θ is the initial concentration of monomers (surface coverage). Equations (4) are preserved if the time t is multiplied with θ. Therefore, after the simulations are completed, we return to the physical time by transforming $t \rightarrow t/\theta$.

It can be shown that the process converges in a probabilistic sense to the solution of the Smoluchowski equations.[45,47] A large number of numerical experiments confirm the convergence of the method for various coagulation kernels used in practice. When using this algorithm, collisions with small probabilities p_{ij} are realized very rarely. The simulations can be essentially accelerated[48] by dividing the set of possible collisions into subsets, each subset containing collisions with close probabilities. Then, the value K_{max} is determined separately for each subset and becomes close to the relevant values of K_{ij}. We use the advanced algorithm in the simulations presented below.

B. Brownian kernel for two-dimensional problem

The kernel K_{ij} describes the rate at which two clusters, containing i and j atoms respectively, meet to form a single cluster containing $i+j$ atoms. In the case of Brownian motion, the original calculation was given by Smoluchowski[41] for the three-dimensional problem. This calculation is usually generalized to a d-dimensional problem and then applied to $d=2$, which gives the simple result $K_{ij} = 2\pi(D_i + D_j)$.[43,49] However, this calculation is valid for $d > 2$, since it is based on the steady-state solution of the diffusion equation that approaches a constant limit (as $1/r^{d-2}$) for $r \rightarrow \infty$. The solution of the 2D diffusion equation behaves as $\ln r$, which results in a divergence that has to be removed.

In more detail, the rate of reaction of a cluster of size i with the clusters of size j in the case of Brownian motion is given by the radial diffusion current of $i$mers to the $j$mer and $j$mers to the $i$mer, $J = J_i + J_j$. The current J_j is given by $J_j = D_j \partial c_j / \partial r$. Here $c_j(r)$ is the concentration of $j$mers at a distance r from the $i$mer. The concentration field is described by the steady-state diffusion equation $\nabla^2 c_j = 0$, with two boundary conditions. First, $c_j(r) = 0$ at $r = R_i + R_j$ meaning that $j$mers disappear by reaction when they reach the surface of $i$mer. The second boundary condition imposed in the three-dimensional case is $c_j(\infty) = n_j$, the mean concentration of $j$mers. This second condition cannot be directly applied in the two-dimensional case, since $c_j(r)$ diverges at infinity.

The solution of the two-dimensional problem can be found in an "effective medium" approach[50] where the concentration field is self-consistently screened by surrounding clusters. The radial flux of $j$mers is given by[50]

$$J_j(r) = D_j n_j \mathcal{K}(r/\xi),\qquad(6)$$

where ξ is a screening length defined below, the function $\mathcal{K}(x)$ is defined as

$$\mathcal{K}(x) = 2\pi x K_1(x)/K_0(x),\qquad(7)$$

$K_0(x)$ and $K_1(x)$ are modified Bessel functions. Then, the coalescence kernel is

$$K_{ij} = (D_i + D_j)\mathcal{K}\left(\frac{R_i + R_j}{\xi}\right).\qquad(8)$$

The (time dependent) screening length ξ is defined by the self-consistency constraint as[50]

$$\xi^{-1} = \int_0^\infty \mathcal{K}(r/\xi) n(r,t) dr.\qquad(9)$$

The problem is highly nonlinear: to find the coagulation coefficient, we have to know the size distribution $n(r,t)$. In our calculations, we obtain the screening length ξ at each time step by solving Eq. (9) for the actual size distribution, and then evaluate the coagulation kernel (8). We find that the
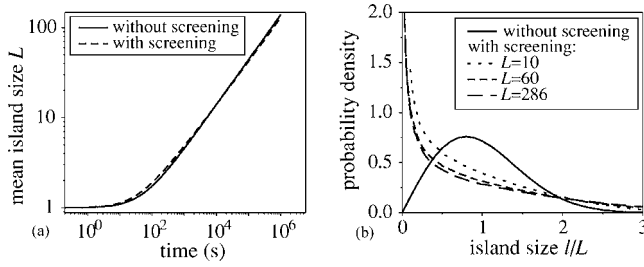
FIG. 5. Time dependence of the mean island size (a) and distribution functions (b) obtained by numerical solution of the Smoluchowski equations for the screening-corrected kernel (8) with the size-independent diffusion coefficients D_j and for a constant kernel $K_{ij}=2\pi(D_i+D_j)$.

screening length is fairly insensitive to the shape of the size distribution. The quantity $\langle r \rangle / \xi$, where $\langle r \rangle$ is the mean size, as a function of the coverage is presented in Fig. 4 of Ref. 50 for some particular island size distribution. We find that the use of this plot, instead of solving Eq. (9), already gives a reasonable accuracy for the island distribution and kinetics. In this approximation, one writes the argument in the form $r/\xi = (r/\langle r \rangle)(\langle r \rangle / \xi)$ and uses the value $\langle r \rangle / \xi$ taken from Ref. 50 for a given coverage.

Figure 5 compares the numerical solution of the Smoluchowski equations with the screening-corrected kernel (8), where the diffusion coefficients are taken size independent, and the solution obtained with the common approximation $K_{ij}=2\pi(D_i+D_j)$, where the diffusion coefficients are also size independent. Figure 5(a) shows that the screening correction of the kernel has rather little effect on the time dependence of the mean island size: the time exponent becomes 0.49, to be compared with 1/2 for the constant kernel case. In contrast, the kernel correction substantially changes the island size distribution, Fig. 5(b). The constant kernel allows analytical solution of the Smoluchowski equation and gives rise to a self-similar size distribution presented below, Eq. (11). This distribution, shown in Fig. 5(b), is peaked at the mean island size. The screening-corrected kernel gives rise to a monotonously decreasing distribution. The distribution changes at the initial stages of coarsening and then reaches a self-similar form with a large fraction of small islands. This distribution is in a good agreement with the results of our atomistic kMC simulations, as compared in Fig. 2(d).

Figure 6 explores the effect of screening for the size-dependent diffusion coefficients (3). Similarly to the case of

the constant diffusion coefficient presented in Fig. 5, the screening has little effect on the time dependence of the mean island size $L(t)$. Both curves in Fig. 6(a), with and without screening, tend to the $t^{1/4}$ asymptotic for the linear island sizes much larger than $\sqrt{k_0}$ in Eq. (3). In this limit, the diffusion coefficients $D_k=D_0 k_0/k$ give rise to the scaling laws (1) and (2) with the exponents $\alpha=2$ and $\beta=1/4$. The island size distributions calculated for the diffusion coefficients (3), Fig. 6(b), also evolve at large times to the limiting distribution corresponding to the case of homogeneous diffusion coefficients. This behavior agrees with the results of Kandel[51] who showed that, in the case of kinetic scaling, the size distribution evolves into a universal dynamically selected distribution. The short-time distribution is forgotten on long times. The evolution of the size distribution on intermediate times, Fig. 6(b), is in a good agreement with the results of out kMC simulations, Fig. 2(d).

For smaller island sizes, the result for the diffusion coefficients (3) notably deviates from that limit. The mean island size reveals a markedly larger time exponent up to a size of about 50. This is in a good agreement with our kMC simulations of the coalescence, Fig. 2(a), where apparent time exponents larger than 1/4 are observed in the size interval available for the atomistic simulations. Numerical solutions of the Smoluchowski equations allow us to extend the analysis to much larger sizes and we find that the asymptotic $t^{1/4}$ law is finally reached. Figure 2(a) also shows that a conclusion regarding the coalescence mechanism, drawn in experiments from a quite limited island size range, may be erroneous.

The effect of screening qualitatively modifies the size distribution at the initial stages of coalescence. Similarly to the case of constant diffusion coefficient, it results in the increase of the fraction of small islands. This is in a good agreement with the results of our kMC calculations, Fig. 2(d). When the mean island size exceeds about 30, the effect of screening diminishes.

C. Analytical solutions

The case of a constant kernel allows an analytical solution of the Smoluchowski equations. We found in Sec. II B that the facetting of the islands gives rise to constant (size independent) diffusion coefficients. Hence, if the screening effect is ignored and the common approximation $K_{ij}=2\pi(D_i+D_j)$
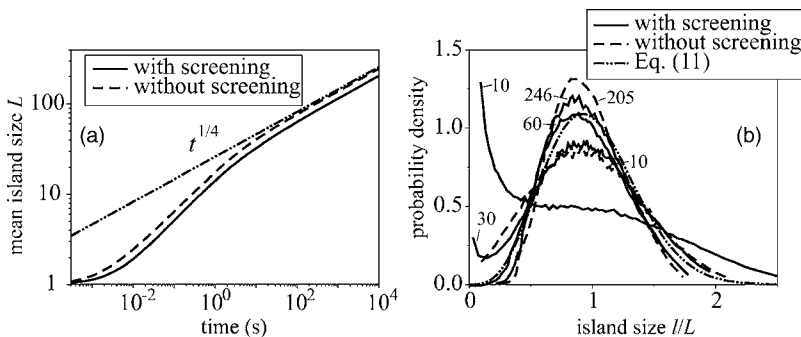

FIG. 6. Time dependence of the mean island size (a) and distribution functions (b) obtained by numerical solution of the Smoluchowski equations for the diffusion coefficient $D_k=D_0/(1+k/k_0)$ and by the approximate formula (11).

is used, an analytical formula to compare with the atomistic kMC simulations can be obtained.

The solution for constant kernel was obtained by Smoluchowski[41] in the form $n_k = n_0 (t/\tau)^{k-1}/(1+t/\tau)^{k+1}$, where n_0 is the initial concentration, $\tau = (Kn_0/2)^{-1}$, and $K = 4\pi D$ is the size-independent kernel. For large times, $t \gg \tau$, the distribution becomes exponential, $n_k = (\tau/t)^2 \exp(-k\tau/t)$. To compare with the kMC results in Fig. 2(d) we have to proceed from the number of vacancies in an island k to the linear size $l_k = \sqrt{k}$. Then, the island size distribution can be written as

$$F(l/L) = \frac{\pi}{2} \frac{l}{L} \exp\left[-\frac{\pi}{4}(l/L)^2 \right]. \qquad (10)$$

The solid line in Fig. 5(b) shows this distribution.

In the case of rounded islands for the bond energy $E_b = 0.2$ eV, an approximate analytical solution of the Smoluchowski equations can be obtained for large times, when the mean number of vacancies in the islands is large compared to k_0 in Eq. (3) and the scaling law (1) with $\alpha = 2$ holds. Then, the kernel K_{ij} becomes homogeneous, $K_{\lambda i, \lambda j} = \lambda^{-\alpha/2} K_{ij}$ for any λ, and the asymptotic size distribution $F(l/L)$ is[31,43,49]

$$F(l/L) = \frac{2W}{\Gamma(1+\alpha/2)}(Wl/L)^{1+\alpha} e^{-(Wl/L)^2}, \qquad (11)$$

where $W = (1+\alpha/2)\Gamma(3/2+\alpha/2)/\Gamma(2+\alpha/2)$. Note that Eq. (10) is a particular case of Eq. (11) with $\alpha = 0$. For $\alpha = 2$, one has $W = 3\sqrt{\pi}/4$. The approximate solution (11), shown in Fig. 6(b), well agrees with the numerical solutions of the Smoluchowski equations.

IV. DISCUSSION

Facetting is the phenomenon that distinguishes the crystalline state from a liquid. Facetting of two-dimensional islands on a crystal surface follows the same general laws as the facetting of a crystal itself.[38] Our kMC simulations show that the Brownian motion of islands and their dynamic coalescence qualitatively change when facetting takes place. The motion of a facetted island consists of a series of discrete jumps, Fig. 3(b), when whole rows of atoms detach from a facet and reattach to another facet. As a result, the diffusion coefficient of an island does not decrease with increasing island size, Fig. 4(b). If the screening effects are not taken into consideration, the dynamic coarsening of facetted islands is described by the scaling laws (1) and (2) with $\alpha = 0$.

In the case of rounded islands at smaller bond energies, the power law (1) for the size dependence of the island diffusion coefficient applies to sufficiently large islands (diameter larger than about $15a$). The exponent $\alpha = 2$ points to a correlated detachment and subsequent reattachment of atoms as the diffusion mechanism.[16–18] However, for small islands, the diffusion coefficient found in the kMC simulations notably deviates from the power law to smaller values, Fig. 4. The origin of the deviation has already been discussed in Sec. II B.

The "effective medium" screening[50] is a peculiarity of diffusion in two dimensions. It removes the singularity of the d-dimensional diffusion equation at $d = 2$. We have derived the kernel (8) for the Smoluchowski equations to describe Brownian motion of islands in two dimensions. The screening has rather little effect on the time dependence of the mean island size but substantially modifies the island size distributions, especially for facetted islands. As a result of screening, the fraction of small islands notably increases. The distribution of facetted islands with size-independent diffusion coefficient becomes monotonously decreasing function. The numerical solution of the equations well agrees with the results of atomistic kMC simulations, Fig. 2(d).

The bond counting ansatz gives us just one relevant dimensionless parameter, the ratio of bond energy to temperature. Facetting takes place when this parameter is large enough. This ansatz, together with the step edge barrier, provides diffusion and coarsening of vacancy islands. The same model applied to adatom islands would cause Ostwald ripening. It is not directly applicable to metal (100) or (111) surfaces, since the experiments[4–14] show that in these systems the detachment of atoms from the island periphery is prohibited and the island motion proceeds due to atom migration along the periphery. More sophisticated models are developed for kMC simulations of these systems.[19–27] However, the experiments on the Ag(110) surface reveal the terrace diffusion as driving force for Brownian motion of vacancy islands.[15] An exponent $\alpha = 2$ in Eq. (1) is found, which agrees with our simulations in the case of small bond energies. The island size independent diffusion coefficient and the monotonously decreasing island size distribution that we obtain for large bond energies were not previously observed.

V. CONCLUSIONS

The appearance of facets in the equilibrium island shape, through either increasing the bond energy or decreasing the temperature, qualitatively change both the Brownian motion of individual islands and their coarsening kinetics. We show by kinetic Monte Carlo simulations that the island diffusion coefficient for facetted islands becomes size independent, the mean island size follows the $L \propto t^{1/2}$ law, and the island size distribution becomes broad and monotonously decreasing.

Numerical solutions of the Smoluchowski equations by a Monte Carlo method allow us to follow the long-term evolution of the island distribution. The kernel of the Smoluchowski equations for Brownian motion in two dimensions is derived in an "effective medium" approach. We find that the screening correction gives rise to a qualitative change of island size distribution but has rather little effect on the time dependence of the average island size. The solutions of the Smoluchowski equations are in a good agreement with the results of our atomistic kinetic Monte Carlo simulations.

[1] W. Ostwald, Z. Phys. Chem. **37**, 385 (1901).

[2] I. M. Lifshitz and V. V. Slyozov, J. Phys. Chem. Solids **19**, 35 (1961).

[3] P. W. Voorhees, J. Stat. Phys. **38**, 231 (1985).

[4] J.-M. Wen, S.-L. Chang, J. W. Burnett, J. W. Evans, and P. A. Thiel, Phys. Rev. Lett. **73**, 2591 (1994).

[5] J. de la Figuera, J. E. Prieto, C. Ocal, and R. Miranda, Solid State Commun. **89**, 815 (1994).

[6] K. Morgenstern, G. Rosenfeld, B. Poelsema, and G. Comsa, Phys. Rev. Lett. **74**, 2058 (1995).

[7] J.-M. Wen, J. W. Evans, M. C. Bartelt, J. W. Burnett, and P. A. Thiel, Phys. Rev. Lett. **76**, 652 (1996).

[8] D. J. Semin, A. Lo, S. E. Roark, R. T. Skodje, and K. L. Rowlen, J. Chem. Phys. **105**, 5542 (1996).

[9] W. W. Pai, A. K. Swan, Z. Zhang, and J. F. Wendelken, Phys. Rev. Lett. **79**, 3210 (1997).

[10] L. Bardotti, M. C. Bartelt, C. J. Jenks, C. R. Stoldt, J.-M. Wen, C.-M. Zhang, P. A. Thiel, and J. W. Evans, Langmuir **14**, 1487 (1998).

[11] G. Rosenfeld, K. Morgenstern, M. Esser, and G. Comsa, Appl. Phys. A **69**, 489 (1999).

[12] C. R. Stoldt, C. J. Jenks, P. A. Thiel, A. M. Cadilhe, and J. W. Evans, J. Chem. Phys. **111**, 5157 (1999).

[13] D. C. Schlößer, K. Morgenstern, L. K. Verheij, G. Rosenfeld, F. Besenbacher, and G. Comsa, Surf. Sci. **465**, 19 (2000).

[14] P. A. Thiel and J. W. Evans, J. Phys. Chem. **104**, 1663 (2000).

[15] K. Morgenstern, E. Lægsgaard, and F. Besenbacher, Phys. Rev. Lett. **86**, 5739 (2001).

[16] C. DeW. Van Siclen, Phys. Rev. Lett. **75**, 1574 (1995).

[17] S. V. Khare, N. C. Bartelt, and T. L. Einstein, Phys. Rev. Lett. **75**, 2148 (1995).

[18] S. V. Khare and T. L. Einstein, Phys. Rev. B **54**, 11752 (1996).

[19] A. F. Voter, Phys. Rev. B **34**, 6819 (1986).

[20] J. M. Soler, Phys. Rev. B **50**, 5578 (1994).

[21] D. S. Sholl and R. T. Skodje, Phys. Rev. Lett. **75**, 3158 (1995).

[22] A. Bogicevic, S. Liu, J. Jacobsen, B. Lundqvist, and H. Metiu, Phys. Rev. B **57**, R9459 (1998).

[23] A. Lo and R. T. Skodje, J. Chem. Phys. **111**, 2726 (1999).

[24] J. Heinonen, I. Koponen, J. Merikoski, and T. Ala-Nissila, Phys. Rev. Lett. **82**, 2733 (1999).

[25] T. Müller and W. Selke, Eur. Phys. J. B **10**, 549 (1999).

[26] S. Pal and K. A. Fichthorn, Phys. Rev. B **60**, 7804 (1999).

[27] G. Mills, T. R. Mattsson, L. Møllnitz, and H. Metiu, J. Chem. Phys. **111**, 8639 (1999).

[28] P. Jensen, N. Combe, H. Larralde, J. L. Barrat, C. Misbah, and A. Pimpinelli, Eur. Phys. J. B **11**, 497 (1999).

[29] D.-J. Liu and J. W. Evans, Phys. Rev. B **66**, 165407 (2002).

[30] P. Meakin, Physica A **165**, 1 (1990).

[31] D. S. Sholl and R. T. Skodje, Physica A **231**, 631 (1996).

[32] A. Lo and R. T. Skodje, J. Chem. Phys. **112**, 1966 (2000).

[33] S. Clarke, M. R. Wilby, D. D. Vvedensky, and T. Kawamura, Phys. Rev. B **40**, 1369 (1989).

[34] S. Clarke, M. R. Wilby, and D. D. Vvedensky, Surf. Sci. **255**, 91 (1991).

[35] A. B. Bortz, M. H. Kalos, and J. L. Lebowitz, J. Comput. Phys. **17**, 10 (1975).

[36] P. A. Maksym, Semicond. Sci. Technol. **3**, 594 (1988).

[37] J. Hoshen and R. Kopelman, Phys. Rev. B **14**, 3438 (1976).

[38] C. Rottman and M. Wortis, Phys. Rev. B **24**, 6274 (1981).

[39] K. Morgenstern, E. Lægsgaard, and F. Besenbacher, Phys. Rev. B **66**, 115408 (2002).

[40] J. M. Soler, Phys. Rev. B **53**, R10540 (1996).

[41] M. von Smoluchowski, Phys. Z. **17**, 585 (1916).

[42] J. D. Langrebe and S. E. Pratsinis, J. Colloid Interface Sci. **139**, 63 (1990).

[43] M. Villarica, M. J. Casey, J. Goodisman, and J. Chaikena, J. Chem. Phys. **98**, 4610 (1993).

[44] K. K. Sabelfeld, *Monte Carlo Methods in Boundary Value Problems* (Springer, New York, 1991).

[45] K. K. Sabelfeld and A. A. Kolodko, Math. Comput. Simul. **61**, 115 (2003).

[46] A. Kolodko and K. Sabelfeld, Monte Carlo Meth. Appl. **9**, 315 (2003).

[47] A. Kolodko, K. Sabelfeld, and W. Wagner, Math. Comput. Simul. **49**, 57 (1999).

[48] K. Sabelfeld and A. Levykin, *Proceedings of V IMACS Seminar on Monte Carlo Methods* (Tallahassee, USA, 2005), p. 52.

[49] R. Jullien, New J. Chem. **14**, 239 (1990).

[50] J. A. Marqusee, J. Chem. Phys. **81**, 976 (1984).

[51] D. Kandel, Phys. Rev. Lett. **79**, 4238 (1997).